A New Old Tale: Dopamine Transporter implications in an animal model of Attention-Deficit Hyperactivity Disorder

Fernández Guillermo[1], Krapacher Favio[1], Ferreras Soledad[1], Quassollo Gonzalo[1], Mari Macarena Mariel[1], Pisano María Victoria[1], Montemerlo Antonella[3], Rubianes María Dolores[3], Bregonzio Claudia[4], Arias, Carlos[1,5] and Paglini María Gabriela[1,2*]

[1]Laboratory of Neurophysiology, Instituto de Investigación Médica Mercedes y Martín Ferreyra, INIMEC-CONICET, Universidad Nacional de Córdoba, Córdoba, Argentina

[2]Virology Institute "Dr. J. M. Vanella", Facultad de Ciencias Médicas, Universidad Nacional de Córdoba, Córdoba, Argentina

[3]Instituto de Investigaciones en Fisicoquímica de Córdoba, INFIQC-CONICET, Facultad de Ciencias Químicas, Universidad Nacional de Córdoba, Córdoba, Argentina

[4]Instituto de Farmacología Experimental Córdoba, IFEC-CONICET, Departamento de Farmacología. Facultad de Ciencias Químicas, Universidad Nacional de Córdoba, Córdoba, Argentina.

[5]Instituto de Investigaciones Psicológicas, IIPSI-CONICET, Facultad de Psicología, Universidad Nacional de Córdoba, Córdoba, Argentina

*** Corresponding author:**
María Gabriela Paglini, Ph.D.
Laboratory of Neurophysiology, Instituto de Investigación Médica Mercedes y Martín Ferreyra, INIMEC-CONICET, Universidad Nacional de Córdoba,
Friuli 2434, 5016 - Córdoba Argentina.
Phone: +54-351-4681465 (ext. 105) Fax: +54-351-4695163.
E-mail: gpaglini@immf.uncor.edu

ABSTRACT

Attention deficit/Hyperactivity disorder (ADHD) is one of the most diagnosed psychiatric disorders nowadays. The core symptoms of the condition include hyperactivity, impulsiveness and inattention. The main pharmacological treatment consists of psychostimulant drugs affecting Dopamine Transporter (DAT) function. We have previously shown that genetically modified mice lacking p35 protein (p35KO), which have reduced Cdk5 activity, present key hallmarks resembling those described in animal models useful for studying ADHD. The p35KO mouse displays spontaneous hyperactivity and shows a calming effect of methylphenidate or amphetamine treatment. Interestingly, dopaminergic neurotransmission is altered in these mice as they have an increased Dopamine (DA) content together with a low DA turnover. This led us to hypothesize that the lack of Cdk5 activity affects DAT expression and/or function in this animal model. In this study, we performed biochemical assays, cell-based approaches, quantitative fluorescence analysis and functional studies that allowed us to demonstrate that p35KO mice exhibit decreased DA uptake and reduced cell surface DAT expression levels in the striatum (STR). These findings are supported by *in vitro* observations in which the inhibition of Cdk5 activity in N2a cells induced a

significant increase in constitutive DAT endocytosis with a concomitant increase in DAT localization to recycling endosomes. Taken together, these data provide strong evidence regarding the role of Cdk5 activity in DAT trafficking and function, thus contributing to the knowledge of DA neurotransmission physiology and also providing therapeutic options for the treatment of DA pathologies such as ADHD.

KEYWORDS

Cdk5/p35; amphetamine; dopamine; endocytosis; endosomes

ABBREVIATIONS

ADHD: Attention deficit/Hyperactivity disorder
DAT: Dopamine Transporter
p35KO: mice lacking p35 protein
WT: wild type mice
DA: Dopamine
STR: striatum
AMPH: amphetamine
ROSCO: roscovitine
AFM: antibody feeding method
DAT-HA: DAT containing a HA epitope in the second extracellular loop
GAPDH: glyceraldehyde 3-phosphate dehydrogenase
MCC: Manders' Colocalization Coefficient

HIGHLIGHTS

- Mice lacking p35 (p35KO) exhibit diminished surface DAT expression in the striatum
- Amperometric experiments show decreased DA uptake in the striatum of p35KO mice
- Cdk5 inhibition increases DAT endocytosis in N2a cells
- Lack of Cdk5 activity increases DAT localization in Rab11 positive endosomes

INTRODUCTION

Attention Deficit Hyperactivity Disorder (ADHD) is a complex, chronic and highly heritable neurodevelopmental disorder with typical onset in childhood and known persistence into adulthood [1]. Like other neuropsychiatric disorders, ADHD presents a spectrum of behavioral alterations with motor hyperactivity features, impulsivity, and/or inattention; offering the diagnostic criteria used for diagnosis [2]. So far, the most effective pharmacotherapy for the disorder comprises long-term treatments with stimulant drugs, such as amphetamine (AMPH) and methylphenidate. These drugs enhance Dopamine (DA) neurotransmission by altering Dopamine Transporter (DAT) normal

function [3–5]. DAT is a key plasma membrane-protein regulating dopaminergic transmission, both spatially and temporally, since it removes released DA from the synaptic cleft by a reuptake mechanism [4]. Given the essential role of DAT in dopaminergic transmission, several studies support its participation in ADHD. Consistently, results obtained using genetically modified animals like DAT knockout (DAT-KO) and cocaine-insensitive DAT (DAT-CI) mice, highlight the role of the transporter in phenotypes related to ADHD [6–12]. Considering that DAT is functional only when it is expressed at the plasma membrane, its surface availability is dynamically and tightly regulated by endocytic trafficking [13–15]. It has been shown that DAT endocytosis is mediated by a clathrin-dependent mechanism [16] and also that Cdk5 kinase plays an essential role in regulating synaptic vesicle endocytosis by phosphorylation of Dynamin I, a protein that participates in clathrin-dependent internalization [17, 18].

Cdk5 is a proline-directed serine/threonine kinase that is activated by its association with a regulatory subunit, either p35 or p39, both of which are brain-specific [19–22]. Cdk5/p35 complex has been involved in several processes, including neuronal migration, axonal and dendritic formation [23–25], neurotransmitter release [26], endocytosis [17, 27], dopaminergic signaling [28] as well as in structural plasticity associated to drugs of abuse [29–31]. Furthermore, Cdk5 activity is tightly regulated in neurons under physiological conditions. Dysregulation of Cdk5 activity gives rise to various neurodevelopmental, neurological and neuropsychiatric disorders, such as Alzheimer's, Parkinson's and Huntington's diseases, ADHD, schizophrenia and stress-induced hippocampal memory deficits, among others [32–36]. In line with these observations, results from our laboratory showed that mice lacking a proper Cdk5 activity recapitulate some key features present in ADHD. By using a mutant mouse lacking p35 (p35KO), which displays reduced Cdk5 activity; we demonstrated that juvenile mice mimic key hallmarks of the human disease, including spontaneous hyperactivity and the decrease of locomotor activity after AMPH or methylphenidate treatment; behavioral response defined as "*paradoxical response to psychostimulants*". Moreover, p35KO mice also exhibited increased DA synthesis and content and decreased DA degradation, resulting in a low DA turnover in basal conditions [37]. These findings together with those previously reported [38] support the validity of the p35KO mouse as an animal model useful for the study of ADHD [39]. Although Cdk5 activity plays a critical role in dopaminergic transmission, dysregulation of Cdk5 and its effects on DAT expression, trafficking and function remain largely unexplored.

In the present study we tested the hypothesis that the lack of p35-activated Cdk5 activity affects DAT expression and/or function in p35KO mice. We demonstrate that dopaminergic activity is altered in the brain of this animal model. Decreased DA uptake and reduced cell surface DAT expression levels were observed in the STR of these mutant animals. These findings are supported by *in vitro* observations, in which the lack of Cdk5 activity induced a significant increase in constitutive DAT endocytosis. Given the central role of DAT in dopaminergic signaling, identifying molecular mechanisms underlying DAT membrane expression, trafficking and function not only

contributes to broaden our understanding of DA neurotransmission but also provides therapeutic options for the treatment of DA pathologies such as ADHD.

MATERIALS AND METHODS

Animals

Wild type (WT) and p35 knockout (p35KO) mice (kind gift of Dr. L.H. Tsai), maintained in a C57BL/6J background via brother-sister mating, were obtained from the vivarium of the INIMEC-CONICET-UNC (Cordoba, Argentina). Mice were weaned at 21 postnatal days and housed up to six per cage under 12 h light /12 h dark cycle, controlled temperature (22°C), and free access to food and water. All experiments were performed using male animals at the age of 24-26 days. All animal procedures and care were approved by the National Department of Animal Care and Health (SENASA–ARGENTINA) and were in compliance with the National Institute of Health general guidelines for the Care and Use of Laboratory Animals. All experimental protocols were reviewed and approved by the Institutional Animal Care and Use Committee (CICUAL) at INIMEC-CONICET-UNC. Efforts were made to minimize animal suffering and to reduce the number of animals used.

Antibodies and Drugs

Sources of primary antibodies: Hemaglutinin (HA), Y11 Santa Cruz Biotechnology (Santa Cruz, CA, USA) (1:400), LAMP-1, H4A3, Iowa Hybridomic bank (Iowa, IA, USA) (1:500), DAT, AB15344 Millipore (Billerica, MA, USA) (1:800, recognizes two bands at 55 and 75 kDa in rat brain tissue and one band at 55 kDa in mouse brain tissue); α-tubulin, DM1A Sigma-Aldrich (St. Louis, MO, USA) (1:5000, recognizes α-subunit of tubulin at 50 kDa); Na^+K^+-ATPase, 464.6(6H) GeneTex (Irvine, CA, USA) (1:50000, recognizes Sodium/Potassium ATPase Alpha-1 at 100 kDa); glyceraldehyde 3-phosphate dehydrogenase (GAPDH) AM4300 Invitrogen (San Diego, CA, USA) (1:5000, recognizes a 37 kDa band corresponding to GAPDH in different cell lines and tissues tested). Sources of secondary antibodies used in western blot: goat anti-mouse IgG IRDye 680/ goat anti-rabbit IgG IRDye 800, Li-Cor Biosciences (Lincoln, NE, USA) (1:10000). Sources of secondary antibodies used in inmunocytochemistry: goat anti-rabbit IgG Alexa Fluor 488 (GAR-488) and goat anti-rabbit IgG Alexa Fluor 568 (GAR-568), ThermoFisher Scientific (Waltham, MA, USA) (see working dilutions in sections below).

D-Amphetamine (AMPH) (Parafarm, Buenos Aires, Argentina) and roscovitine (ROSCO) (Calbiochem, San Diego, CA, USA) were used in this study.

Cell line and DNA constructs

Mouse Neuro 2a (N2a) cells (CCL-131), acquired from American Type Culture Collection (Manassas, VA) were cultured at 37°C, 5% CO_2 in Dulbecco's Modified Eagle Medium (DMEM, ThermoFisher Scientific, Waltham, MA, USA) supplemented with fetal bovine serum (FBS) 5% (NATOCOR, Córdoba, Argentina), glutamine 2 mM, penicillin 10,000 U/ml, and streptomycin 10 mg/ml (ThermoFisher Scientific, Waltham, MA, USA).

N2a cells were transiently transfected using Lipofectamine 2000 (ThermoFisher Scientific, Waltham, MA, USA) according to the manufacturer's recommendations.

For antibody feeding method (AFM) experiments, N2a cells were transfected with a DAT containing a HA epitope (YPYDVPDASL) in the second extracellular loop (DAT-HA) [3]. This construct was a kind gift from Dr. Susan Amara (National Institute of Mental Health, Bethesda, MD, USA). In colocalization experiments, early and recycling endosomes markers, Rab5-GFP and Rab11-GFP, respectively, were used. These plasmids were a kind gift from Dr. José Luis Daniotti (CIQUIBIC-Universidad Nacional de Córdoba, Córdoba, Argentina).

Experimental Procedures

Surface DAT biotinylation assay

For the assessment of surface DAT levels in synaptosomes from striatal tissue, crude synaptosomal fractions were obtained as described [29]. Briefly, naïve p35KO and WT mice were sacrificed by cervical dislocation and the STRs were quickly dissected out on ice-cooled dishes and homogenized in ice-cold Sucrose Buffer (0.32 M sucrose, 10 mM HEPES and 1 mM EDTA pH 7.4, 1 µg/ml aprotinin, 1 µg/ml leupeptin, 100 µg/ml PMSF, 1 µg/ml pepstatin, and 0.2 mM sodium orthovanadate; all chemicals were from Sigma-Aldrich, St. Louis, MO, USA) using a small Potter glass-Teflon homogenizer. The resulting homogenate was passed three times trough a 30G syringe. The sample was then centrifuged twice at 1000 G for 5 min at 4 °C. The supernatant (total homogenate, HT) was centrifuged at 12500 G for 20 min at 4°C. The resulting pellet (crude synaptosomal fraction) was resuspended in 1 ml of PBS/Ca^+/Mg^+ buffer and protein content was quantified by DC protein assay kit (Bio-Rad Laboratory, Hercules, CA, USA). 500 µg of synaptosomes were incubated 60 min at 4 °C with sulfo-NHS-biotin (1.5 mg/ml) in 500 µl of PBS/Ca^+/Mg^+ pH 7.4 (ThermoFisher Scientific, Waltham, MA, USA). Biotinylation reaction was quenched by incubating the synaptosomes with 1 vol of PBS containing glycine 100 mM for 15 min. Subsequently, the sample was washed twice with the same buffer. Synaptosomes were then resuspended in lysate buffer (1% Triton X-100, 1% Nonidet P-40, 10% glycerol in TBS buffer pH 7.4 supplemented with 1 µg/ml aprotinin, 1 µg/ml leupeptin, 100 µg/ml PMSF, 1 µg/ml pepstatin and 0.2 mM sodium orthovanadate; all chemicals were from Sigma-Aldrich, St. Louis, MO, USA). After that, samples were sonicated twice (10 sec x 30 mA). An aliquot of this fraction was separated (synaptosomal total DAT). Samples (300 µg) were then incubated with streptavidin beads 100 µl (ThermoFisher Scientific, Waltham, MA, USA) overnight at 4° C. Beads were washed five times with lysate buffer and biotinylated proteins were eluted with Laemmli buffer (62,5 mM Tris-HCl, pH 6.8, 20% glycerol, 2% SDS, and 5% β-mercaptoethanol) for 30 min at RT.

Surface DAT biotynilation after AMPH treatment

Striatal synaptosomes (500 µg) from p35KO and WT mice, following the same procedure as describe above, were resuspended in Krebs Ringer Buffer (KRB) containing 145 mM NaCl, 2.7 mM KCl, 1.2 mM KH_2PO_4, 1.2 mM $CaCl_2$, 1 mM $MgCl_2$, 10 mM glucose, 0.255 mM ascorbic acid, and 24.9 mM $NaHCO_3$. Samples were then incubated with AMPH (10 µM) or VEH for 30 min at 37°C in

gentle agitation. The reaction was then stopped with two ice-cold KRB washes. Subsequently, the biotinylation procedure was carried out as described in the previous section.

Western Blot

Protein immunoblotting was performed as previously described [31]. HT (25 µg), synaptosomal total DAT (25 µg) and half of each biotinylated fraction were separated into 10% SDS-PAGE gels electrophoresis and transferred to nitrocellulose membranes (Bio-Rad Laboratory, Hercules, CA, USA). Subsequently, membranes were first incubated 60 min at RT with blocking buffer (5% skim milk in TBS tween 0,05%) and then incubated over night at 4 °C in agitation with the following antibodies: anti-DAT, anti-tubulin, anti-Na-K-ATPase and anti-GAPDH. Membranes were then washed and incubated 60 min at RT with the appropriate Licor IRDye secondary antibody. Protein signals were detected using an Odissey scanner (LI-COR Biosciences, Lincoln, NE, USA). Western blot bands analyzed by densitometry were quantified with ImageJ.

Dopamine uptake in p35KO and WT mice STRs: amperometric experiments

Naïve p35KO and WT mice were sacrificed by cervical dislocation and the STRs were quickly dissected on ice, chopped with a razor blade and homogenized in 1.1 ml of cold KRB saturated with a gas mixture of 95% O_2 and 5% CO_2. Subsequently, DA uptake was carried out as described below.

Electrochemical procedure: DA uptake was evaluated by amperometric measurements with a glassy carbon electrode (GCE) modified with a dispersion of multi walled carbon nanotubes (Nano-Lab, Waltham, MA, USA) functionalized with polietilenimine (Sigma, St. Louis, MO, USA) (CNT-PEI) as sensing platform. The electrochemical measurements were performed with TEQ-04 potentiostats. The electrodes were inserted into the cell (BAS, Model MF-1084) through holes in its Teflon cover. A platinum and an Ag/AgCl wire in 3M KCl were used as counter and reference electrodes, respectively. All potentials measured by the working electrode (BAS, Model RE-5B) were referred to the Ag/AgCl electrode. A magnetic stirrer provided the convective transport during the amperometric measurements.

The experiments were carried out in a KRB solution saturated with a gas mixture (95% O_2 and 5% CO_2) at 37°C, by applying +0.250 V and monitoring the current response in the absence or in the presence of 500 µl of homogenized striatal samples. The oxidation current signal value was measured initially (i_0) and after 300 seconds (i_{300}) of the addition of 5.0 x 10^{-7} M DA (Sigma, St. Louis, MO, USA). The decrease in the oxidation current signal was used to calculate DA pmols taken up by DAT. DA reuptake was finally expressed as pmol of DA/µg of total protein/min. In order to perform the measurements as quickly as possible, the total protein content was measured after the experiment.

The glassy carbon electrode modified with carbon nanotubes dispersed in polyethylenimine (GCE/CNT-PEI) was prepared as described by Rubianes and Rivas [40]. GCE was polished with alumina slurries of 1.00, 0.30 and 0.05 µm for 1 min each and sonicated in water for 30 s, and then modified by drop coating with an aliquot of 20 µL of CNT-PEI and allowed to dry for 90 min. The

dispersion of CNT-PEI was obtained by sonicating 1.0 mg of MWCNTs within 1.0 mL of 1.0 mg/mL PEI solution (prepared in 50:50 v/v ethanol/water) for 5.0 min with an ultrasonic probe.

Antibody feeding method (AFM) and pharmacological treatments

N2a cells were grown in coverslips and transfected with DAT-HA. 24 hs after transfection, cells were incubated with anti-HA (Y11) 20 µg/ml and ROSCO 10 µM or DMSO (vehicle) in FBS-free DMEM for 30 min at 18 °C. After that, DMSO treated cells were incubated with AMPH 10 µM (AMPH group) or VEH (Control group), meanwhile, ROSCO treated cells were maintained with this drug (ROSCO group) for 60 min at 37 °C. Subsequently, cells were washed with PBS and fixed for 20 min with 4% paraformaldehyde (Riedel-de Haën, Sigma-Aldrich Laborchemikalien GmbH, Seelze, Germany) in 100 mM Phosphate Buffered Saline (PBS) at room temperature (RT). In order to label surface DAT-HA, cells were incubated with a secondary anti-rabbit antibody Alexa Fluor-568 (80 µg/ml) in PBS containing Bovine Serum Albumin (BSA) 1% at RT for 60 min. Cells were then washed with PBS and permeabilized with Triton X-100 0.2% BSA 1% in PBS at RT. Cells were then incubated with a secondary anti-rabbit antibody Alexa Fluor-488 (2 µg/ml) in PBS containing BSA 1% at RT for 60 min to label endocyted DAT-HA. After incubation, cells were washed and mounted on slides using FluorSave (Calbiochem Merck KgaA, Darmstadt, Germany).

Subsequently, high-resolution images of N2a cells were acquired in FV-1000 laser-scanning confocal microscope (Olympus, Tokyo, Japan) in two channels (excitation wavelength: 494/578, emission wavelength: 517/603) using an oil immersion 63X (NA 1.4) objective (PlanApo, Olympus). Optical sections were acquired at 0.5 µm intervals from top to bottom of cells and data were imported into ImageJ (U.S. National Institutes of Health, Bethesda, MD, USA) for analysis. The average of fluorescence intensity from three medial Z-stacks was used for quantification. Background intensity was subtracted from images prior to quantification.

Colocalization experiments and pharmacological treatments

N2a cells were grown in coverslips and co-transfected with plasmids encoding DAT-HA and Rab5-GFP or Rab11-GFP. After 24 hs of expression, cells were incubated with ROSCO (10 µM) or AMPH (10 µM) for 30 min in FBS free DMEM. Cultures were immediately washed with PBS and fixed for 20 min with 4% paraformaldehyde in 100 mM PBS at RT. Subsequently, cells were permeabilized with Triton X-100 0.2 mM in PBS. After three PBS washes, cells were incubated with BSA 5% in PBS for 60 min and then incubated 60 min at RT with primary antibody anti-HA (Y11) to label DAT-HA. Cells were then incubated with anti-rabbit Alexa-Fluor 568 (1:400) for 60 min, washed three times and mounted onto slides using FluorSave.

In DAT/LAMP-1 colocalization experiments, cells were transfected with DAT-HA. After 24 hs of expression cells were incubated with ROSCO (10 µM) for 30 min and then processed as described above. Endogenous LAMP-1 was labeled with a primary antibody anti-LAMP-1 and a secondary antibody AlexaFluo-488 (1:400).

Subsequently, images were acquired in FV-300 laser-scanning confocal microscope (Olympus, Tokyo, Japan) in two channels (excitation wavelength: 494/578, emission wavelength: 517/603)

using an oil immersion 63X (NA 1.4) objective (PlanApo, Olympus). In these experiments, optical sections were recorded in 0.25 µm intervals and data were imported to ImageJ for quantitative colocalization analysis. Given that serum deprivation in N2a cells promotes the development of lamellar structures similar to neurites [41], fluorescence intensity of each endosomal marker protein was quantified only in neurite-like processes. In view of the low number of LAMP-1 positive vesicles in neurite-like processes, for LAMP-1/DAT colocalization analysis, quantification was done using the whole cell.

Images were deconvoluted using PSF Generator and Deconvolution lab plug-in (Biomedical Imaging group) [42]. For each cell, a focal plane with well-defined endomembrane structures was selected for analysis and colocalization was quantified in the 15 µm distal portion of neurites with the ImageJ plugin JaCoP [43]. Threshold for DAT and endomembrane marker signals were defined for each cell in order to avoid colocalization overestimation. The colocalization coefficient selected for the analysis was Manders M1 (MCC). This was defined as the summed intensities of pixels from endosomal marker images for which the intensity in DAT images was above zero compared to the total intensity in the endosomal marker images [43].

Statistical analysis

Statistical analyses were performed using R software [44]. Assumptions of homoscedasticity and normality were tested using Levene and Shapiro-Wilks tests, respectively. In those cases in which the assumptions were met, we used unpaired student *t*-test, one-way or two-way ANOVA as appropriate followed by Tukey post-hoc test (Type I error set at 0.05). Data that did not meet these assumptions were analyzed with the non-parametric tests Kruskal-Wallis followed by Mann-Whitney's test when necessary.

RESULTS

Mice lacking Cdk5-activator p35 display decreased DA uptake in the striatum

Alterations in DA balance have been related to a broad spectrum of neurological and psychiatric disorders such as Parkinson´s and Huntington´s diseases, schizophrenia, substance abuse and ADHD, among others. We have previously shown that DA content is dramatically augmented in the STR of mutant mice lacking p35, which display reduced Cdk5 activity. In spite of the high DA concentration, these mutant mice produce less DOPAC than their WT littermates, resulting in a low DA turnover in basal conditions [37]. Considering these results and the fact that DA homeostasis is maintained mainly by DAT through monoamine reuptake, we analyzed DAT expression and function in the STR of these mice.

We first determined DAT expression levels in total striatal homogenates and synaptosomes from juvenile naïve WT and p35 KO mice. Western blots analyses showed no differences in DAT expression levels in total homogenates (t-test: $t = 0.53972$, $df = 6$, $p = 0.6088$) or synaptosomal fractions (t-test: $t = 0.03702$, $df = 6$, $p = 0.9717$) between WT and p35KO mice (Fig. 1a).

Simultaneously, to test the functional consequences of decreased Cdk5 activity in DA uptake, we performed amperometry experiments in the STR of p35KO and WT mice. Homogenized STR tissues from both genotypes were incubated with 5.0 x 10^{-7} M of DA at 37º C in KRB and DA uptake was recorded for 5 min. Data were expressed as pmol of DA/µg/min (see Materials and Methods). The quantitative analysis showed a dramatic decrease of 50% in DA uptake in p35KO preparations compared to WT controls (Fig. 1b) (t-test: t = -3.1773, df = 6, $p < 0.05$).
Even though total DAT expression levels remained invariable in both genotypes, DAT activity in the STR of p35KO mice was significantly lower than in WT controls, suggesting that the reduced Cdk5 activity exhibited by p35KO mice might affect transporters density at the plasma membrane.

Mutant p35 KO mice exhibit reduced DAT cell surface expression in the striatum

Taking into account the decreased DA reuptake observed in STR of p35KO animals, we investigate whether the reduced Cdk5 activity exhibited by p35KO mice affects DAT surface expression. For this purpose, cell surface biotinylation experiments were performed to examine DAT levels at the plasma membrane of striatal synaptosomes obtained from WT and p35KO mice. Quantitative analysis of total extracts and surface fractions (biotinylated DAT/total DAT ratios) showed a 60 % reduction in the amount of surface DAT in p35KO mice compared to WT (Fig. 1c) (t-test: t = -3.007, df = 5, $p < 0.05$). As shown above, total DAT levels in the synaptosomal fraction remained invariable between genotypes (t-test: t = 2.180, df = 5, p = 0.081) (Fig. 1c). It is important to note the lack of GAPDH in biotinylated fractions ensuring they are free from intracellular contaminants (Fig. 1c).
We have previously shown that AMPH treatment induces a paradoxical calming effect on locomotor activity in p35KO mice and restores STR DA content to WT levels [37]. Since AMPH exposure triggers DAT internalization [45], we next analyzed the effect of this psychostimulant on DAT surface expression levels in striatal synaptosomes from p35KO and WT mice. Quantitative analysis revealed that 30 min of AMPH (10 µM) exposure significantly decreased DAT surface levels in synaptosomes from WT animals (two-way ANOVA, $F_{(1,11)} = 17.684$ $p < 0.01$) (Fig. 1d). However, incubation of synaptosomes from p35KO mice with AMPH did not affect DAT surface expression levels (p35KO vehicle compared to p35KO AMPH $p = 0.490$). Notably, vehicle incubated p35KO striatal synaptosomes displayed surface DAT expression levels similar to those observed in AMPH stimulated WT synaptosomes (WT AMPH vs p35KO Veh, $p = 0.171$). Finally, no significant statistical differences were observed in total DAT levels in synaptosomal fractions from both genotypes, regardless of the treatment given (two-way ANOVA, $F_{(1,11)} = 2.651$, $p = 0.131$) (Fig. 1d).
Taken together, our results demonstrate that mutant mice lacking p35, which display reduced Cdk5 activity, exhibit low DA uptake along with diminished surface DAT expression levels.

Figure 1. about here.

Inhibition of Cdk5 increases DAT endocytosis in N2a cells

The dynamic balance between endocytosis and recycling is known to determine DAT surface levels. Hence, we performed in vitro experiments in N2a cells to determine whether Cdk5 participates in DAT internalization. To this end, we used the antibody-feeding method (AFM), a quantitative immunofluorescence technique that had been previously validated [3, 46]. The experimental approach consisted in the pharmacological inhibition of Cdk5 kinase activity with the specific inhibitor roscovitine (ROSCO) in DAT-HA transfected cells. Since DAT endocytosis triggered by AMPH had been reported in a broad variety of cell lines, we used this psychostimulant as a positive control of DAT internalization [47–49]. The results showed that ROSCO (10 μM) or AMPH (10 μM) incubations in DAT-HA transfected N2a cells, significantly raised intracellular/surface DAT-HA ratios, demonstrating that inhibition of Cdk5 activity or AMPH treatment increased DAT endocytosis (Kruskal-Wallis test: $H = 8.76$, $df = 2$, $p < 0.05$) (Fig. 2a and b). Consistent with these observations, the expression of shRNA-mediated Cdk5 knockdown also increased intracellular/surface DAT-HA ratios (data not shown). These results suggest that Cdk5 is a negative regulator of constitutive DAT endocytosis and support functional and biochemical results obtained in p35KO mice

Figure 2. about here**.**

Inhibition of Cdk5 activity arrests DAT in recycling endosomes

Taking into account that DAT endocytic pathway is highly regulated and involves several intermediate organelles, it is important to examine the fate of internalized DAT following Cdk5 activity inhibition and AMPH exposure in cultured N2a cells. For this purpose, we designed experiments using fluorescence confocal microscopy for quantitative colocalization analysis of co-transfected N2a cells with DAT-HA with either Rab5-GFP or Rab11-GFP, early and recycling endosome markers, respectively [50]. Using Manders' Colocalization Coefficient (MCC) [51], we observed a substantial constitutive colocalization (vehicle-control conditions) of intracellular DAT-HA with either Rab5-GFP or Rab11-GFP, which had similar MCC values (0.131 ± 0.019 and 0.154 ± 0.018, respectively) (Fig. 3a and b). Following 30 min of AMPH (10 μM) treatment, a significant amount of DAT-HA colocalized with both endosomal compartments (t-test: $t = -3.491$, $df = 28$, $p < 0.01$ for Rab5 positive endosomes and Kruskal-Wallis test: $H = 10.961$, $df = 1$, $p < 0.01$ for Rab11 positive endosomes). Noteworthy, AMPH incubation increased DAT-HA/Rab11-GFP MCC by approximately two-fold compared to DAT-HA/Rab5-GFP and almost three-fold compared to constitutively internalized DAT (Fig. 3b). These data are consistent with the enhanced DAT endocytosis observed in AMPH treated N2a cells (Fig. 2) and support the notion that internalized DAT following AMPH exposure traffics to early and recycling endosomes.

Figure 3. about here.

Interestingly, when N2a cells co-transfected with DAT-HA and Rab5-GFP or Rab11-GFP were treated with ROSCO to inhibit Cdk5 activity, there was a dramatic change in DAT subcellular localization. In addition, a substantial amount of DAT-HA was observed only in recycling endosomes (Fig. 4). DAT-HA/Rab11-GFP MCC significantly increased compared to the vehicle-control condition, whereas DAT-HA/Rab5-GFP MCC remained invariable after the inhibition treatment (t-test: $t = -2.869$, $df = 35$, $p < 0.01$ for recycling Rab11 endosomes and $t = -0.253$, $df = 46$, $p = 0.800$ for early Rab5 endosomes) (Fig. 4a and b).

Considering these results, and the fact that constitutively internalized DAT is also sorted to late endosomes/lysosomes [14], we next analyzed whether the fate of internalized DAT after Cdk5 activity inhibition is destined for degradation. To this end, we evaluated colocalization of DAT-HA and LAMP1, a late endosome/lysosome marker, in N2a cells exposed to ROSCO or Vehicle for 30 min. According to the MCC quantification analysis, no significant differences were observed between DAT-HA/LAMP1 under Cdk5 inhibition and the vehicle-control condition (t-test: $t = 1.120$, $df = 18$, $p = 0.277$) (Fig. 4c).

These data suggest that pharmacological inhibition of Cdk5 activity increases constitutive DAT endocytosis, resulting in an accumulation of the transporter in recycling endosomes, maintaining the normal trafficking to the lysosomal degradative pathway.

Taken all together, our results demonstrate that mutant mice lacking p35, which display reduced Cdk5 activity, exhibit low DA uptake along with diminished surface DAT expression levels. These findings are supported by *in vitro* observations in which the lack of Cdk5 activity induced a significant increase in DAT constitutive endocytosis with a concomitant loss of DAT from the cell surface.

Figure 4. about here.

DISCUSSION

ADHD is one of the most common psychiatric conditions affecting both children and adults worldwide [52]. The high ADHD prevalence has raised the interest of the scientific community to understanding its neurobiological bases. In this context, animal models of human diseases play a critical role in the exploration and characterization of the pathophysiology and represent a very useful tool in preclinical research to identify, evaluate and validate novel therapeutic agents and treatments. We have previously shown that the mutant mouse lacking p35 protein, which has reduced Cdk5 activity, presents key hallmarks that resemble those of ADHD, thus supporting its validity as a genetically modified animal model useful for studying the disorder [37–39]. The p35KO mouse displays spontaneous hyperactivity and responds paradoxically to psychostimulant treatments. Noteworthy, dopaminergic neurotransmission is altered in p35KO mice, showing increased TH protein levels, increased DA content and decreased DA degradation which result in a

low neurotransmitter turnover [37]. These features led us to hypothesize that the lack of p35-activated Cdk5 activity affects DAT expression and/or function in this animal model. In this study, we performed biochemical assays, functional studies, cell-based approaches and quantitative fluorescence analysis that allowed us to demonstrate that p35KO mice exhibit low DA uptake along with diminished surface DAT expression levels in the STR. These findings are supported by *in vitro* observations in which the inhibition of Cdk5 activity in N2a cells induced a significant increase in constitutive DAT endocytosis, with a concomitant increase of DAT localization to recycling endosomes.

The results obtained in p35KO mice show that the lack of p35-activated Cdk5 activity down-regulates striatal cell surface DAT without affecting the total expression levels of the transporter. Considering that pharmacological inhibition of Cdk5 kinase activity induces DAT internalization in N2a cells (Fig. 2), it is likely that an increase in DAT endocytic-rate underlies the reduced DAT surface levels observed in these mice. In addition, in previous studies we have demonstrated that inhibition of Cdk5 or p35 expression or its inactivation with ROSCO or olomoucine results in a decreased exocytic vesicles transport from the Golgi apparatus [53], suggesting that the lack of Cdk5 activity may provoke an impairment of DAT trafficking to the cell surface. Furthermore, DAT losses from the plasma membrane are not due to blocking of newly synthesized DAT, because total DAT expression levels remained invariable between both genotypes.

As expected, the reduction of striatal surface DAT in p35KO mice results in decreased DAT function. Besides, our results are in agreement with previous reports on mutant mice expressing 10% of WT DAT levels (DAT knockdown) as DA uptake in these mice is also significantly lower than in WT controls [54]. The present results are also consistent with the finding that PKCβ-knockout mice display reduced surface DAT expression levels and reduced DA uptake with no differences in total DAT expression in the STR [55]. Decrease in DA uptake was also observed in rat striatal synaptosomes incubated *in vitro* with different Cdk5 inhibitors, in a concentration- and time-dependent manner [56]. Thus, our data suggest that p35-activated Cdk5 activity is important for the maintenance of surface DAT in basal conditions, as evidenced by the reduced surface DAT expression level and DA uptake in p35KO mice compared to WT, without genotype differences in total DAT expression levels. The spontaneous hyperactivity observed in p35KO mice [37] is consistent with the low surface DAT expression levels and reduced DA uptake reported here. Besides, our data are also in agreement with the increased basal locomotor activity described in DAT knockout and DAT knockdown mice [54, 57].

The fact that AMPH belongs to the first line of ADHD pharmacological treatments, improving executive function, attentional focus and calming locomotor activity [58], led a number of pharmacological studies to address the effect of AMPH on DAT expression and activity. In this sense, AMPH treatment of striatal synaptosomes from WT mice reduced surface DAT expression levels. Likewise, the reduction in surface DAT upon exposure to AMPH has also been reported in rat and mouse STRs and in heterologous expression systems [13, 45, 47, 55, 59–61]. Incubation

of striatal synaptosomes from p35KO mice with AMPH elicits a decrease in surface DAT expression compared to vehicle. Even though this decrease was not statistically significant, it suggests that the lack of AMPH effect could reflect a floor effect, where surface DAT levels could not be reduced further or where the effect of AMPH is dependent on DAT superficial levels. Interestingly, vehicle-incubated p35KO striatal synaptosomes display low surface DAT expression levels similar to those observed in AMPH stimulated WT synaptosomes. Studies carried out in DAT transgenic mice have indicated that AMPH behavioral effect is dependent on the degree of DAT expression [62, 63]. Our results support previous findings showing that AMPH has a calming effect on p35KO mice and suggest that AMPH locomotion effect is dependent on DAT surface expression. Previous studies have reported that the serotoninergic system is involved in the psychostimulant calming effect observed in animal models useful for the study of ADHD. For instance, methylendioximethamphetamine (MDMA), which has a higher effect on serotoninergic relative to dopaminergic neurons, decreases locomotor activity in DAT-knockdown mice [62]. Moreover, it has been shown that the serotonin inhibitor fluoxetine has a calming effect on DAT-KO mice [57]. Therefore, given the low DAT surface expression in p35KO mice, the serotoninergic system is likely to be involved in the AMPH paradoxical effect observed in these animals.

Performing *in vitro* experiments, using N2a cells, we demonstrated that pharmacological inhibition of Cdk5 kinase activity with the widely used inhibitor ROSCO (10 μM) induces DAT internalization (Fig. 2). Other reports using higher doses of the inhibitor in non-neural cells showed that ROSCO at 30 μM in porcine aortic endothelial (PAE) cells does not accelerate DAT endocytosis or modify cell surface DAT levels [56]. These differences may be the result of the effect of ROSCO concentration on the intrinsic transport properties of DATs, on the activity of other kinases that regulate surface DAT expression [64, 65] and/or the experimental model used. Notwithstanding these differences, our results suggest that Cdk5 could be acting as a negative regulator of constitutive DAT endocytosis, supporting functional and biochemical results obtained in p35KO mice. It is well known that the amount of cell surface DAT is the result of a dynamic balance between endocytosis and recycling to the membrane, processes that are highly regulated by a variety of proteins. In this sense, it has been demonstrated that constitutive and substrate induced DAT internalization are clathrin-dependent processes [16, 47, 66] where dynamin catalyzes the pinching-off clathrin-coated pits from the plasma membrane [67]. Interestingly, previous studies have reported that in cultured hippocampal neurons, Cdk5-mediated phosphorylation of dynamin I impairs its association with amphiphysin I, resulting in synaptic vesicle endocytosis inhibition. Moreover, evidences obtained in p35KO mice support these findings since vesicle endocytosis is enhanced in hippocampal neurons from these animals [18]. Our *in vitro* and *in vivo* results reinforce and extend these observations since p35KO mice exhibit a reduced cell surface DAT expression in the STR (Fig. 1c).

Because internalized DAT-containing vesicles have a specific postendocytic sorting [3, 14], we analyzed the internalization pathways of the transporter under Cdk5 inhibition or AMPH treatment

in N2a cells. We used early and recycling endosome marker proteins fused to GFP to carry out quantitative colocalization analyses. Under steady-state conditions, we observed a substantial colocalization of DAT with both, early (Rab5 positive) and recycling (Rab11 positive) endosomes. These results on constitutive DAT trafficking in N2a cells are consistent with previous reports demonstrating that internalized DAT is sorted to the recycling pathways [16, 68]. It is well known that AMPH is one of DAT targeted drugs commonly prescribed for ADHD treatment [69–71]. This psychostimulant competes with DA for DAT's active site and promotes DA reverse transport, increasing extracellular DA levels [72, 73]. Besides, and considering that it had been reported that AMPH triggers DAT endocytosis in a broad variety of cell lines [47–49], we analyzed the fate of internalized DAT following AMPH exposure in cultured N2a cells. AMPH incubation for 30 min not only increases DAT endocytosis, but also significantly increases DAT localization to early and recycling endosomes (Fig. 3). It is important to note that AMPH raises DAT-HA/Rab11-GFP MCC to a greater extent than that of DAT-HA/Rab5-GFP. This supports the notion that internalized DAT, following AMPH exposure, traffics to the recycling endosome pathway for surface reinsertion, as previously shown in cultured MN9D and HEK293 cell lines and in embryonic rat primary mesencephalic cultures [3].

We next examined the fate of internalized DAT following pharmacological inhibition of Cdk5 kinase activity in cultured N2a cells. Surprisingly, ROSCO (10 μM) treatment enhances only DAT-recycling endosomes colocalization. DAT-HA/Rab11-GFP MCC increases significantly compared to vehicle-control condition, whereas DAT-HA/Rab5-GFP and DAT-HA/LAMP1 (Fig. 4) MCC remain invariable after the inhibition treatment. Altogether, these data demonstrate that the lack of Cdk5 activity induces the sorting of constitutive internalized-DAT to the recycling pathway. However, trafficking to the lysosomal degradative pathway remains unaffected. The large amount of DAT in recycling endosomes after Cdk5 activity inhibition suggests that Cdk5 participates in the regulation of the dynamic balance between constitutive DAT endocytosis and recycling to the membrane. Some lines of evidence support this notion. It has been previously shown that the small GTPase Rab11 and its effectors control recycling endosomes trafficking and also transporters and receptors replenishment at the plasma membrane [74]. Moreover, a recent report showed that Cdk5/p35 complex regulates the Rab11-effector GRAB by phosphorylation, modulating the transport of Rab11-dependent endosomes [75]. Furthermore, the final step of the trafficking process is the docking and fusion of Rab11-positive vesicles at the plasma membrane, where the involvement of Cdk5 has already been demonstrated. In addition, it was reported that Cdk5-mediated phosphorylation of Munc18 promotes the Stx3-SNAP25 complex formation to allow the assembly of functional SNARE fusion machinery for regulated vesicle docking and fusion at the plasma membrane [76, 77].

Taken all together these data provide strong evidence regarding the role of Cdk5/p35 in DAT expression and function, thus contributing to the knowledge of ADHD pathophysiology.

CONCLUSIONS

Overall, this study provides new insights regarding the role of Cdk5/p35 complex in the regulation of dopaminergic transmission, as it shows a novel function of this complex as a modulator of DAT membrane expression, trafficking and function. A greater understanding of these processes and their mechanistic details may lead to generate novel therapeutic strategies for the treatment of dopaminergic pathologies, such as ADHD. Nowadays, it is known that ADHD is a chronic condition that continues into adulthood and psychostimulant treatments are often prescribed for years. Therefore, the availability of animal models are invaluable tools to unscramble the complicated nature of complex psychiatric disorders like ADHD, and provide a great opportunity to screen potential therapeutic strategies.

FUNDING

This work was supported by grants from: Agencia Nacional de Promoción Científica y Tecnológica, Argentina (FONCyT PICT/11-0892 and PICT/15-2416); Consejo Nacional de Investigaciones Científicas y Técnicas - CONICET PIP-2014 and Secretaria de Ciencia y Tecnología, Universidad Nacional de Córdoba (PRIMAR-TP Nº 32520170100046CB).

CONFLICTS OF INTEREST/COMPETING INTERESTS

All authors declare that the research was conducted in the absence of any commercial or financial relationships that could be construed as a potential conflict of interest.

ACKNOWLEDGMENTS

We thank Maria Julia Cambiasso for her all-encompassing support, Andrea Pelegrini for technical assistance, Mariana Bollo, Pablo Helguera and Mariano Bisbal for generously providing some antibodies. We would particularly like to thank Damian Revillo and Evelin Cotella for helpful discussions, Patricio Pereyra for his assistance with animal husbandry and the vivarium technicians for their daily support. Confocal microscopy was performed at the Centro de Micro y Nanoscopía de Córdoba, CEMINCO-CONICET-Universidad Nacional de Córdoba, Córdoba, Argentina.

AUTHOR CONTRIBUTIONS

All authors were responsible for the design of the study. GF, FK and SF performed the experimental procedures and collected data. MVP and CA conducted statistical data analysis. GF and GQ performed imaging analysis. GF and MMM conducted biochemical essays. AM and MDR performed amperometric experiments. CB and CA contributed ideas and comments. GF and MGP interpreted the findings and drafted the manuscript. Supervision and project administration were done by MGP and funding's acquisition by MGP and CA. All authors critically reviewed contents and approved the final version for publication.

REFERENCES

1. Sharma A, Couture J (2014) A Review of the Pathophysiology, Etiology, and Treatment of Attention-Deficit Hyperactivity Disorder (ADHD). Ann Pharmacother 48:209–225. https://doi.org/10.1177/1060028013510699
2. American Psychiatric Association (2013) DSM-5 Diagnostic Classification. In: Diagnostic and Statistical Manual of Mental Disorders. American Psychiatric Association
3. Hong WC, Amara SG (2013) Differential targeting of the dopamine transporter to recycling or degradative pathways during amphetamine- or PKC-regulated endocytosis in dopamine neurons. FASEB J 27:2995–3007. https://doi.org/10.1096/fj.12-218727
4. German CL, Baladi MG, McFadden LM, et al (2015) Regulation of the Dopamine and Vesicular Monoamine Transporters: Pharmacological Targets and Implications for Disease. Pharmacol Rev 67:1005–1024. https://doi.org/10.1124/pr.114.010397
5. Faraone S V., Perlis RH, Doyle AE, et al (2005) Molecular genetics of attention-deficit/hyperactivity disorder. Biol Psychiatry 57:1313–1323. https://doi.org/10.1016/j.biopsych.2004.11.024
6. Leo D, Gainetdinov RR (2013) Transgenic mouse models for ADHD. Cell Tissue Res 354:259–271. https://doi.org/10.1007/s00441-013-1639-1
7. Hawi Z, Cummins TDR, Tong J, et al (2015) The molecular genetic architecture of attention deficit hyperactivity disorder. Mol Psychiatry 20:289–297. https://doi.org/10.1038/mp.2014.183
8. Li Z, Chang S hua, Zhang L yan, et al (2014) Molecular genetic studies of ADHD and its candidate genes: A review. Psychiatry Res.
9. Sakrikar D, Mazei-Robison MS, Mergy MA, et al (2012) Attention Deficit/Hyperactivity Disorder-Derived Coding Variation in the Dopamine Transporter Disrupts Microdomain Targeting and Trafficking Regulation. J Neurosci 32:5385–5397. https://doi.org/10.1523/JNEUROSCI.6033-11.2012
10. O'Neill B, Gu HH (2013) Amphetamine-induced locomotion in a hyperdopaminergic ADHD mouse model depends on genetic background. Pharmacol Biochem Behav 103:455–459. https://doi.org/10.1016/j.pbb.2012.09.020
11. Napolitano F, Bonito-Oliva A, Federici M, et al (2010) Role of aberrant striatal dopamine D1 receptor/cAMP/protein kinase A/DARPP32 signaling in the paradoxical calming effect of amphetamine. J Neurosci 30:11043–56. https://doi.org/10.1523/JNEUROSCI.1682-10.2010
12. Federici M, Latagliata EC, Ledonne A, et al (2014) Paradoxical Abatement of Striatal Dopaminergic Transmission by Cocaine and Methylphenidate. J Biol Chem 289:264–274. https://doi.org/10.1074/jbc.M113.495499
13. Melikian HE (2004) Neurotransmitter transporter trafficking: endocytosis, recycling, and regulation. Pharmacol Ther 104:17–27. https://doi.org/10.1016/j.pharmthera.2004.07.006
14. Eriksen J, Bjørn-Yoshimoto WE, Jørgensen TN, et al (2010) Postendocytic sorting of constitutively internalized dopamine transporter in cell lines and dopaminergic neurons. J Biol Chem 285:27289–27301. https://doi.org/10.1074/jbc.M110.131003
15. Bermingham DP, Blakely RD (2016) Kinase-dependent Regulation of Monoamine Neurotransmitter Transporters. Pharmacol Rev 68:888–953. https://doi.org/10.1124/pr.115.012260
16. Sorkina T, Hoover BR, Zahniser NR, Sorkin A (2005) Constitutive and Protein Kinase C-Induced Internalization of the Dopamine Transporter is Mediated by a Clathrin-Dependent Mechanism. Traffic 6:157–170. https://doi.org/10.1111/j.1600-0854.2005.00259.x
17. Tan TC, Valova V a, Malladi CS, et al (2003) Cdk5 is essential for synaptic vesicle endocytosis. Nat Cell Biol 5:701–710. https://doi.org/10.1038/ncb1020
18. Tomizawa K, Sunada S, Lu YF, et al (2003) Cophosphorylation of amphiphysin I and dynamin I by Cdk5 regulates clathrin-mediated endocytosis of synaptic vesicles. J Cell Biol 163:813–824. https://doi.org/10.1083/jcb.200308110
19. Ishiguro K, Kobayashi S, Onion A, et al (1994) Identification of the 23 kDa subunit of tau protein kinase II as a putative activator of cdk5 in bovine brain. FEBS Lett. https://doi.org/10.1016/0014-5793(94)80501-6
20. Tang D, Yeung J, Lee KY, et al (1995) An isoform of the neuronal cyclin-dependent kinase 5 (Cdk5) activator. J Biol Chem 270:26897–26903. https://doi.org/10.1074/jbc.270.45.26897

21. Lew J, Wang JH (1995) Neuronal cdc2-like kinase. Trends Biochem. Sci.
22. Tsai L-H, Delalle I, Caviness VS, et al (1994) p35 is a neural-specific regulatory subunit of cyclin-dependent kinase 5. Nature 371:419–423. https://doi.org/10.1038/371419a0
23. Paglini G, Pigino G, Kunda P, et al (1998) Evidence for the participation of the neuron-specific CDK5 activator P35 during laminin-enhanced axonal growth. J Neurosci 18:9858–9869
24. Shah K, Lahiri DK (2017) A Tale of the Good and Bad: Remodeling of the Microtubule Network in the Brain by Cdk5. Mol Neurobiol 54:2255–2268. https://doi.org/10.1007/s12035-016-9792-7
25. Shah K, Rossie S (2018) Tale of the Good and the Bad Cdk5: Remodeling of the Actin Cytoskeleton in the Brain. Mol Neurobiol 55:3426–3438. https://doi.org/10.1007/s12035-017-0525-3
26. Kim SH, Ryan TA (2010) CDK5 Serves as a Major Control Point in Neurotransmitter Release. Neuron 67:797–809. https://doi.org/10.1016/j.neuron.2010.08.003
27. Nguyen C, Bibb JA (2003) Cdk5 and the mystery of synaptic vesicle endocytosis. J Cell Biol 163:697–699. https://doi.org/10.1083/jcb.200310038
28. Svenningsson P, Nishi A, Fisone G, et al (2004) DARPP-32: An Integrator of Neurotransmission. Annu Rev Pharmacol Toxicol 44:269–296. https://doi.org/10.1146/annurev.pharmtox.44.101802.121415
29. Mlewski EC, Krapacher FA, Ferreras S, Paglini G (2008) Transient Enhanced Expression of Cdk5 Activator p25 after Acute and Chronic d -Amphetamine Administration. Ann N Y Acad Sci 1139:89–102. https://doi.org/10.1196/annals.1432.039
30. Mlewski EC, Arias C, Paglini G (2016) Association between the expression of amphetamine-induced behavioral sensitization and Cdk5/p35 activity in dorsal striatum. Behav Neurosci 130:. https://doi.org/10.1037/bne0000118
31. Ferreras S, Fernández G, Danelon V, et al (2017) Cdk5 Is Essential for Amphetamine to Increase Dendritic Spine Density in Hippocampal Pyramidal Neurons. Front Cell Neurosci 11:. https://doi.org/10.3389/fncel.2017.00372
32. Shah K, Lahiri DK (2014) Cdk5 activity in the brain-multiple paths of regulation. J Cell Sci 127:2391–400. https://doi.org/10.1242/jcs.147553
33. Ikiz B, Przedborski S (2008) Previews A Sequel to the Tale of p25 / Cdk5 in Neurodegeneration. 731–732. https://doi.org/10.1016/j.neuron.2008.11.020
34. Kawauchi T (2014) Cdk5 regulates multiple cellular events in neural development, function and disease. Dev Growth Differ 56:335–348. https://doi.org/10.1111/dgd.12138
35. Piccini A, Perlini LE, Cancedda L, et al (2015) Phosphorylation by PKA and Cdk5 Mediates the Early Effects of Synapsin III in Neuronal Morphological Maturation. J Neurosci 35:13148–13159. https://doi.org/10.1523/JNEUROSCI.1379-15.2015
36. Rei D, Mason X, Seo J, et al (2015) Basolateral amygdala bidirectionally modulates stress-induced hippocampal learning and memory deficits through a p25/Cdk5-dependent pathway. Proc Natl Acad Sci U S A. https://doi.org/10.1073/pnas.1415845112
37. Krapacher FA, Mlewski EC, Ferreras S, et al (2010) Mice lacking p35 display hyperactivity and paradoxical response to psychostimulants. J Neurochem 114:203–14. https://doi.org/10.1111/j.1471-4159.2010.06748.x
38. Drerup JM, Hayashi K, Cui H, et al (2010) Attention-deficit/hyperactivity phenotype in mice lacking the cyclin-dependent kinase 5 cofactor p35. Biol Psychiatry 68:1163–1171. https://doi.org/10.1016/j.biopsych.2010.07.016
39. de la Peña JB, dela Peña IJ, Custodio RJ, et al (2017) Exploring the Validity of Proposed Transgenic Animal Models of Attention-Deficit Hyperactivity Disorder (ADHD). Mol Neurobiol 55:3739–3754. https://doi.org/10.1007/s12035-017-0608-1
40. Rubianes MD, Rivas GA (2007) Dispersion of multi-wall carbon nanotubes in polyethylenimine: A new alternative for preparing electrochemical sensors. Electrochem commun 9:480–484. https://doi.org/10.1016/j.elecom.2006.08.057
41. López-Maderuelo MD, Fernández-Renart M, Moratilla C, Renart J (2001) Opposite effects of the Hsp90 inhibitor Geldanamycin: induction of apoptosis in PC12, and differentiation in N2A cells. FEBS Lett 490:23–7. https://doi.org/10.1016/s0014-5793(01)02130-5
42. Sage D, Donati L, Soulez F, et al (2017) DeconvolutionLab2: An open-source software for deconvolution microscopy. Methods 115:28–41. https://doi.org/10.1016/j.ymeth.2016.12.015

43. Bolte S, Cordelières FP (2006) A guided tour into subcellular colocalization analysis in light microscopy. J Microsc 224:213–32. https://doi.org/10.1111/j.1365-2818.2006.01706.x
44. R Core Team (2020) R: A language and environment for statistical computing
45. Johnson LA, Furman CA, Zhang M, et al (2005) Rapid delivery of the dopamine transporter to the plasmalemmal membrane upon amphetamine stimulation. Neuropharmacology 49:750–758. https://doi.org/10.1016/j.neuropharm.2005.08.018
46. Sorkina T, Miranda M, Dionne KR, et al (2006) RNA interference screen reveals an essential role of Nedd4-2 in dopamine transporter ubiquitination and endocytosis. J Neurosci 26:8195–8205. https://doi.org/10.1523/JNEUROSCI.1301-06.2006
47. Saunders C, Ferrer J V., Shi L, et al (2000) Amphetamine-induced loss of human dopamine transporter activity: An internalization-dependent and cocaine-sensitive mechanism. Proc Natl Acad Sci 97:6850–6855. https://doi.org/10.1073/pnas.110035297
48. Sorkina T, Doolen S, Galperin E, et al (2003) Oligomerization of dopamine transporters visualized in living cells by fluorescence resonance energy transfer microscopy. J Biol Chem 278:28274–28283. https://doi.org/10.1074/jbc.M210652200
49. Chi L, Reith ME a (2003) Substrate-induced trafficking of the dopamine transporter in heterologously expressing cells and in rat striatal synaptosomal preparations. J Pharmacol Exp Ther 307:729–736. https://doi.org/10.1124/jpet.103.055095
50. Stenmark H (2009) Rab GTPases as coordinators of vesicle traffic. Nat Rev Mol Cell Biol 10:513–25. https://doi.org/10.1038/nrm2728
51. Dunn KW, Kamocka MM, McDonald JH (2011) A practical guide to evaluating colocalization in biological microscopy. AJP Cell Physiol 300:C723–C742. https://doi.org/10.1152/ajpcell.00462.2010
52. Sayal K, Prasad V, Daley D, et al (2018) ADHD in children and young people: prevalence, care pathways, and service provision. The Lancet Psychiatry
53. Paglini G, Peris L, Diez-Guerra J, et al (2001) The Cdk5-p35 kinase associates with the Golgi apparatus and regulates membrane traffic. EMBO Rep 2:1139–44. https://doi.org/10.1093/embo-reports/kve250
54. Zhuang X, Oosting RS, Jones SR, et al (2001) Hyperactivity and impaired response habituation in hyperdopaminergic mice. Proc Natl Acad Sci U S A 98:1982–7. https://doi.org/10.1073/pnas.98.4.1982
55. Chen R, Furman CA, Zhang M, et al (2009) Protein Kinase Cβ Is a Critical Regulator of Dopamine Transporter Trafficking and Regulates the Behavioral Response to Amphetamine in Mice. J Pharmacol Exp Ther 328:912–920. https://doi.org/10.1124/jpet.108.147959
56. Price DA, Sorkin A, Zahniser NR (2009) Cyclin-dependent kinase 5 inhibitors: inhibition of dopamine transporter activity. Mol Pharmacol 76:812–823. https://doi.org/10.1124/mol.109.056978
57. Gainetdinov RR (1999) Role of Serotonin in the Paradoxical Calming Effect of Psychostimulants on Hyperactivity. Science (80-) 283:397–401. https://doi.org/10.1126/science.283.5400.397
58. Briars L, Todd T (2016) A Review of Pharmacological Management of Attention-Deficit/Hyperactivity Disorder. J Pediatr Pharmacol Ther 21:192–206. https://doi.org/10.5863/1551-6776-21.3.192
59. Gulley JM, Doolen S, Zahniser NR (2002) Brief, repeated exposure to substrates down-regulates dopamine transporter function in Xenopus oocytes in vitro and rat dorsal striatum in vivo. J Neurochem 83:400–411. https://doi.org/10.1046/j.1471-4159.2002.01133.x
60. Zahniser NR, Sorkin A (2004) Rapid regulation of the dopamine transporter: Role in stimulant addiction? Neuropharmacology 47:80–91. https://doi.org/10.1016/j.neuropharm.2004.07.010
61. Boudanova E, Navaroli DM, Melikian HE (2008) Amphetamine-induced decreases in dopamine transporter surface expression are protein kinase C-independent. Neuropharmacology 54:605–612. https://doi.org/10.1016/j.neuropharm.2007.11.007
62. Cagniard B, Sotnikova TD, Gainetdinov RR, Zhuang X (2014) The Dopamine Transporter Expression Level Differentially Affects Responses to Cocaine and Amphetamine. J Neurogenet 28:112–121. https://doi.org/10.3109/01677063.2014.908191
63. Salahpour A, Ramsey AJ, Medvedev IO, et al (2008) Increased amphetamine-induced hyperactivity and reward in mice overexpressing the dopamine transporter. Proc Natl Acad

Sci U S A 105:4405–10. https://doi.org/10.1073/pnas.0707646105
64. Meijer L, Borgne A, Mulner O, et al (1997) Biochemical and Cellular Effects of Roscovitine, a Potent and Selective Inhibitor of the Cyclin-Dependent Kinases cdc2, cdk2 and cdk5. Eur J Biochem 243:527–536. https://doi.org/10.1111/j.1432-1033.1997.t01-2-00527.x
65. Morón J a, Zakharova I, Ferrer J V, et al (2003) Mitogen-activated protein kinase regulates dopamine transporter surface expression and dopamine transport capacity. J Neurosci 23:8480–8488
66. Carvelli L, Morón JA, Kahlig KM, et al (2002) PI 3-kinase regulation of dopamine uptake. J Neurochem 81:859–869. https://doi.org/10.1046/j.1471-4159.2002.00892.x
67. Damke H, Baba T, Warnock DE, Schmid SL (1994) Induction of mutant dynamin specifically blocks endocytic coated vesicle formation. J Cell Biol 127:915–934. https://doi.org/10.1083/jcb.127.4.915
68. Loder MK, Melikian HE (2003) The dopamine transporter constitutively internalizes and recycles in a protein kinase C-regulated manner in stably transfected PC12 cell lines. J Biol Chem 278:22168–74. https://doi.org/10.1074/jbc.M301845200
69. Bitter I, Angyalosi A, Czobor P (2012) Pharmacological treatment of adult ADHD. Curr. Opin. Psychiatry
70. Vaughan BS, March JS, Kratochvil CJ (2012) The evidence-based pharmacological treatment of paediatric ADHD. Int J Neuropsychopharmacol 15:27–39. https://doi.org/10.1017/S1461145711000095
71. Minzenberg MJ (2012) Pharmacotherapy for Attention-Deficit/Hyperactivity Disorder: From Cells to Circuits. Neurotherapeutics 9:610–621. https://doi.org/10.1007/s13311-012-0128-7
72. Fleckenstein AE, Volz TJ, Riddle EL, et al (2007) New Insights into the Mechanism of Action of Amphetamines. Annu Rev Pharmacol Toxicol 47:681–698. https://doi.org/10.1146/annurev.pharmtox.47.120505.105140
73. Kahlig KM, Binda F, Khoshbouei H, et al (2005) Amphetamine induces dopamine efflux through a dopamine transporter channel. Proc Natl Acad Sci U S A 102:3495–500. https://doi.org/10.1073/pnas.0407737102
74. Johnson JL, He J, Ramadass M, et al (2016) Munc13-4 Is a Rab11-binding Protein That Regulates Rab11-positive Vesicle Trafficking and Docking at the Plasma Membrane. J Biol Chem 291:3423–3438. https://doi.org/10.1074/jbc.M115.705871
75. Furusawa K, Asada A, Urrutia P, et al (2017) Cdk5 Regulation of the GRAB-Mediated Rab8-Rab11 Cascade in Axon Outgrowth. J Neurosci 37:790–806. https://doi.org/10.1523/JNEUROSCI.2197-16.2016
76. Liu Y, Ding X, Wang D, et al (2007) A mechanism of Munc18b-syntaxin 3-SANP25 complex assembly in regulated epithelial secretion. FEBS Lett 581:4318–4324. https://doi.org/10.1016/j.febslet.2007.07.083
77. Tomizawa K, Ohta J, Matsushita M, et al (2002) Cdk5/p35 regulates neurotransmitter release through phosphorylation and downregulation of P/Q-type voltage-dependent calcium channel activity. J Neurosci 22:2590–7. https://doi.org/20026252

FIGURE LEGENDS

Figure 1 p35KO mice exhibit decreased DA uptake and DAT cell surface expression in the STR (a) Representative western immunoblots showing DAT expression levels in total STR homogenates and synaptosomal fractions from WT and p35KO mice (measured by DAT/Tubulin ratio; mean ± SEM, Student t-test, n= 4). (b) DAT activity in STR homogenates from p35KO and WT mice. Striatal tissue was homogenized in KRB and DA uptake assay was performed by an amperometric technique using a glassy carbon electrode. Results are expressed as pmol of DA/µg of protein/min (mean ± SEM, Student t-test, * indicates $p < 0.05$, n= 4). (c) Surface protein biotinylation experiments in striatal synaptosomes from WT and p35KO mice. Representative

western immunoblots of biotinylated (surface) and non-biotinylated (total) DAT expression levels in striatal synaptosomes from WT and p35KO mice (upper panels). Surface DAT levels were measured as surface/total DAT ratio. Note the decreased expression of DAT in the surface fraction of p35KO mice. Medial panels show surface and total Na^+/K^+ ATPase expression levels and bottom panels, GAPDH levels. Total DAT levels were quantified measuring total DAT/GAPDH ratio (mean ± SEM, Student t-test, $*p < 0.05$, n= 3-4). (d) AMPH effect on DAT surface expression in striatal synaptosomes from WT and p35KO mice. Representative western blots of biotinylated (surface) and non-biotinylated (total) DAT expression in striatal synaptosomes from animals of both genotypes incubated for 30 min with AMPH or VEH. DAT surface expression was measured as surface/total ratio. Total DAT expression levels were analyzed by total DAT/GAPDH ratio. (mean ± SEM, two-way ANOVA followed by Tukey test, * indicates $p < 0.05$; n = 3-5).

Figure 2 Inhibition of Cdk5 activity or AMPH treatment increases DAT internalization in N2a cells (a) Cell surface DAT-HA was labeled by anti-HA11 followed by drug-induced internalization. Representative images of control (CTRL), ROSCO (10 μM) and AMPH (10 μM) treated N2a cells. Left panels show surface DAT-HA signal labeled with goat anti-rabbit-568, middle panels show internalized DAT-HA labeled with goat anti-rabbit-488 and right panels show the overlay of the two channels; scale bar = 10 μm. (b) Fluorescence quantification from confocal stacks between internalized DAT and surface DAT (mean ± SEM, Kruskal-Wallis test followed by Mann-Whitney U comparison tests; * indicates $p < 0.05$, n= 25-28 cells for each condition).

Figure 3 AMPH treatment increases DAT localization to early and recycling endosomes N2a cells expressing DAT-HA and Rab5-GFP or Rab11-GFP were incubated with AMPH (10 μM) or vehicle (CTRL) for 30 min and colocalization between DAT and endosome markers was quantified. Representative Rab5-GFP/DAT-HA (a) and Rab11-GFP/DAT-HA (b) fluorescence signal images. Left panels show endosomal markers, medial panels show DAT-HA signal, and right panels, the overlay of the two channels. Bottom-right sections are enlarged images of boxed areas. Arrowheads indicate colocalized voxels. Scale bar = 10 μm. Bar graphs represent the quantification of fluorescence colocalization between DAT and endosome markers using Manders' Colocalization Coefficient (MCC). (mean ± SEM, Student t-test in a and Kruskal-Wallis test in b, * indicates $p < 0.05$, n=10-16 processes for each condition).

Figure 4 Cdk5 inhibition increases DAT localization only to recycling endosomes N2a cells expressing DAT-HA or DAT-HA together with either Rab5-GFP or Rab11-GFP were treated with ROSCO (10 μM) or vehicle (CTRL) for 30 min. Then, colocalization between DAT with endosome and lysosome (LAMP-1) markers was quantified. Representative fluorescence signal images of Rab5-GFP/DAT-HA (a), Rab11-GFP/DAT-HA (b) and LAMP-1/DAT-HA (c). Left panels show endosomal and lysosomal markers, medial panels show DAT-HA signal, and right panels, the

overlay of the two channels. Bottom-right sections are enlarged images of boxed areas. Arrowheads indicate colocalized voxels. Scale bar = 10 μm. Bar graphs represent quantification of fluorescence colocalization between DAT and endosome (a and b) and lysosome markers (c) using Manders' Colocalization Coefficient (MCC) (mean ± SEM, Student t-test, * indicates $p < 0.05$ n=15-25 processes for each condition in a and b and n= 9-11 cells for each condition in c).

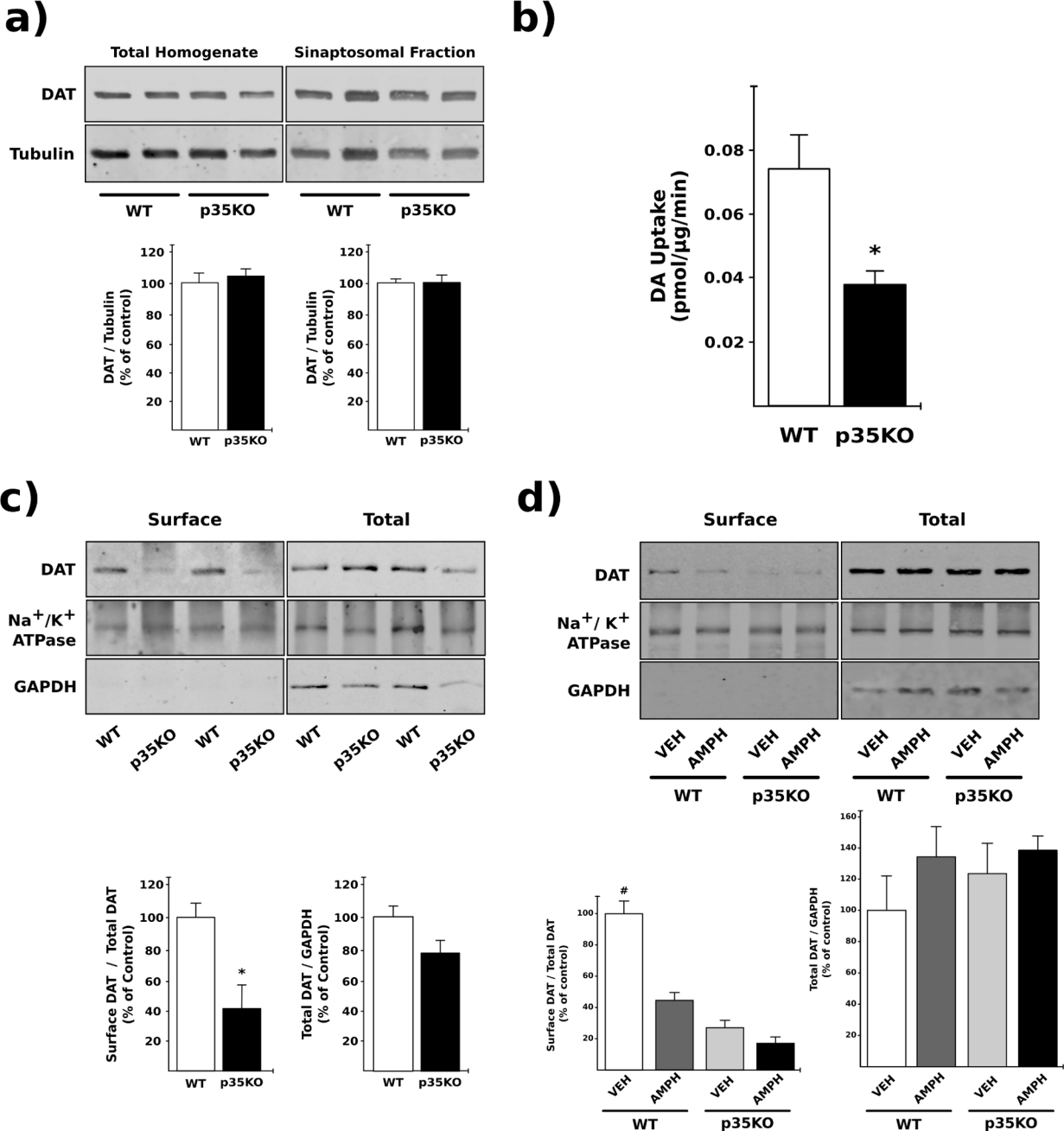
a)
Total Homogenate
Sinaptosomal Fraction
DAT
Tubulin
WT
p35KO
WT
p35KO
DAT / Tubulin (% of control)
120
100
80
60
40
20
WT
p35KO
DAT / Tubulin (% of control)
120
100
80
60
40
20
WT
p35KO
b)
DA Uptake (pmol/µg/min)
0.08
0.06
0.04
0.02
*
WT
p35KO
c)
Surface
Total
DAT
Na+/K+ ATPase
GAPDH
WT
p35KO
WT
p35KO
WT
p35KO
WT
p35KO
Surface DAT / Total DAT (% of Control)
120
100
80
60
40
20
*
WT
p35KO
Total DAT / GAPDH (% of Control)
120
100
80
60
40
20
WT
p35KO
d)
Surface
Total
DAT
Na+/ K+ ATPase
GAPDH
VEH
AMPH
VEH
AMPH
VEH
AMPH
VEH
AMPH
WT
p35KO
WT
p35KO
Surface DAT / Total DAT (% of control)
#
100
80
60
40
20
VEH
AMPH
VEH
AMPH
WT
p35KO
Total DAT / GAPDH (% of control)
160
140
120
100
80
60
40
20
VEH
AMPH
VEH
AMPH
WT
p35KO

a)

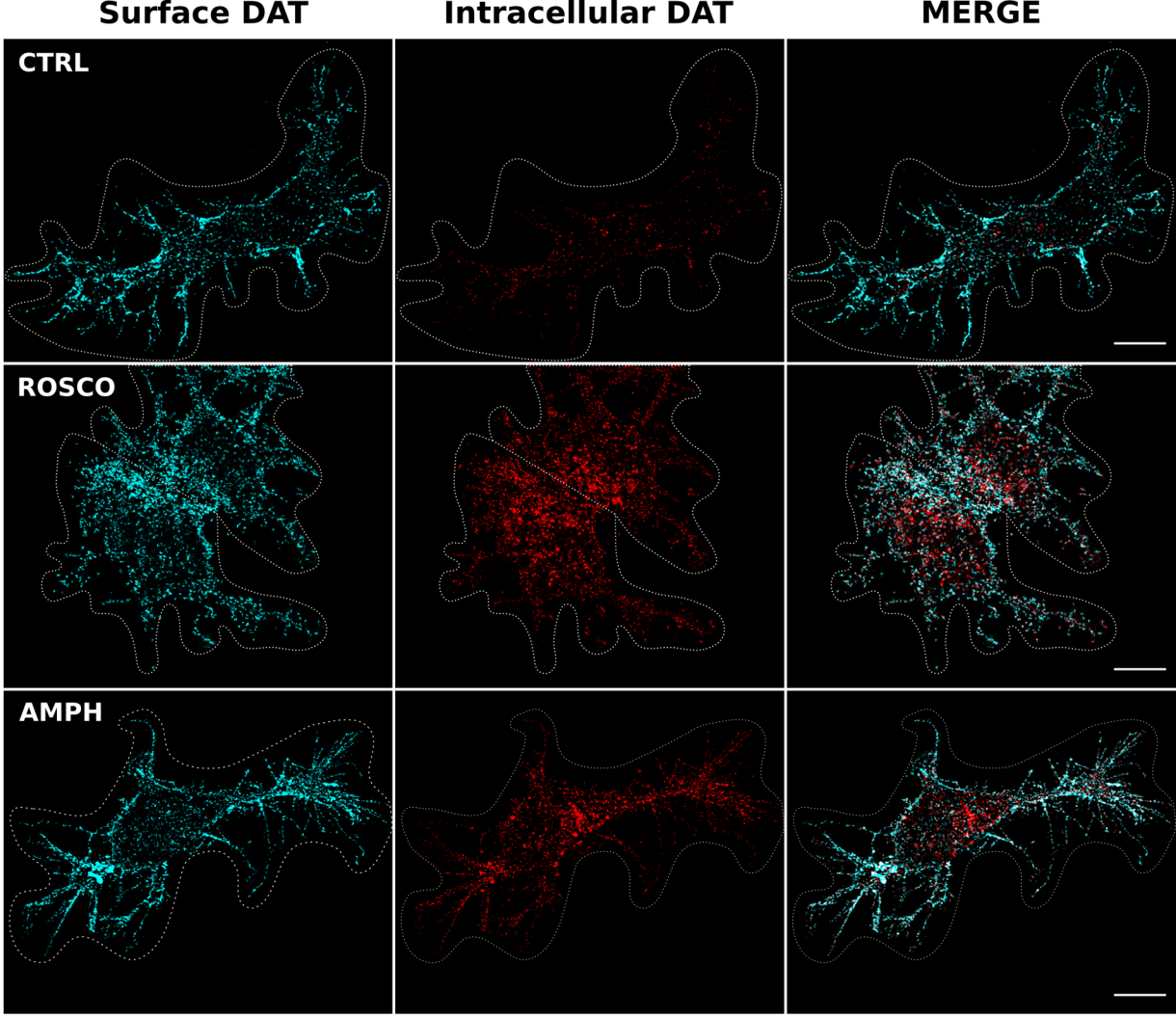
Surface DAT
Intracellular DAT
MERGE
CTRL
ROSCO
AMPH

b)

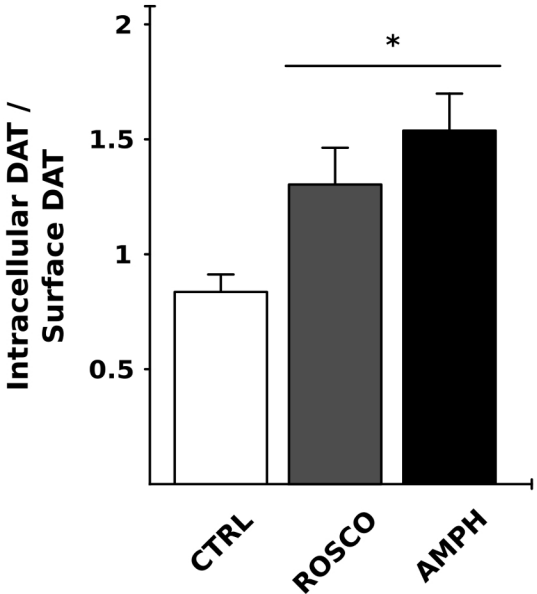
Intracellular DAT / Surface DAT
2
1.5
1
0.5
*
CTRL
ROSCO
AMPH

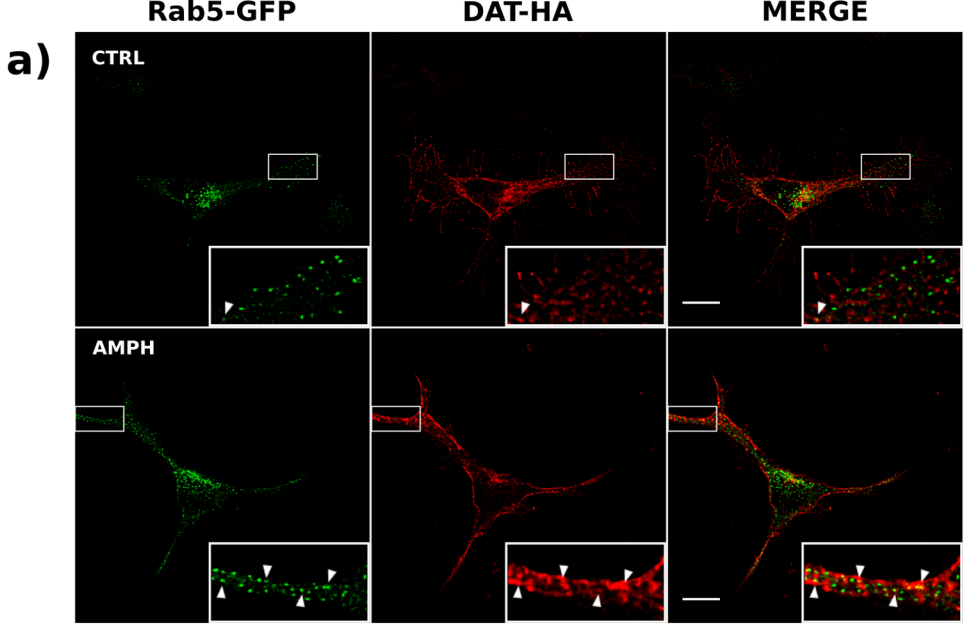
a)
Rab5-GFP
DAT-HA
MERGE
CTRL
AMPH

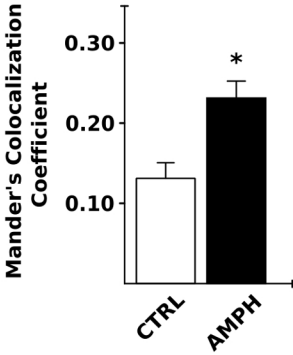
Mander's Colocalization Coefficient
0.30
0.20
0.10
*
CTRL
AMPH

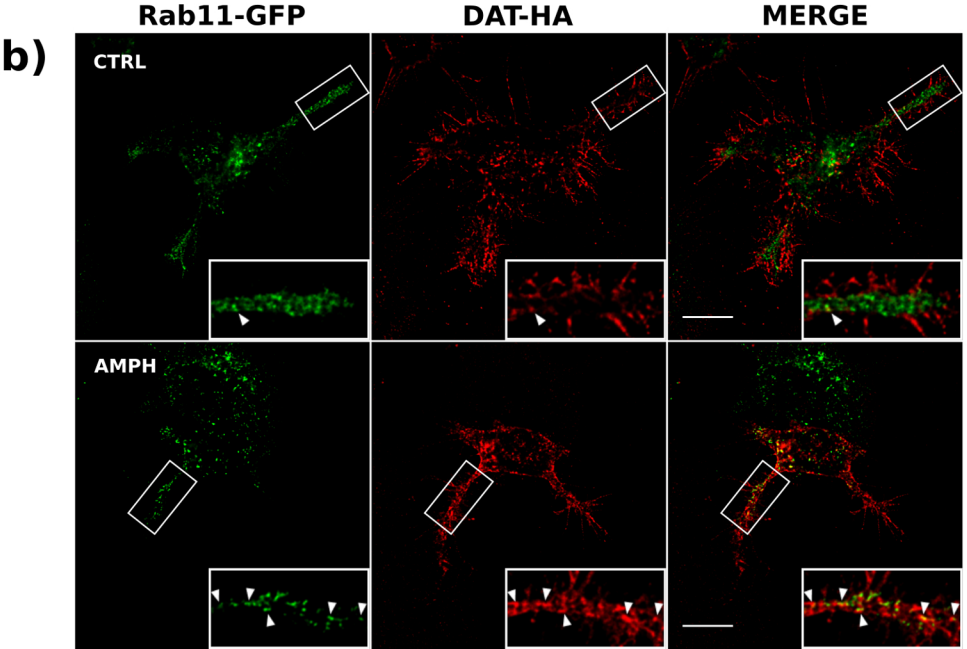
b)
Rab11-GFP
DAT-HA
MERGE
CTRL
AMPH

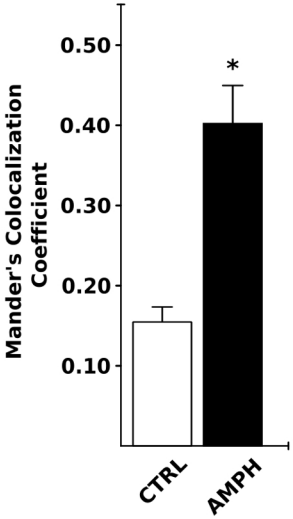
Mander's Colocalization Coefficient
0.50
0.40
0.30
0.20
0.10
*
CTRL
AMPH

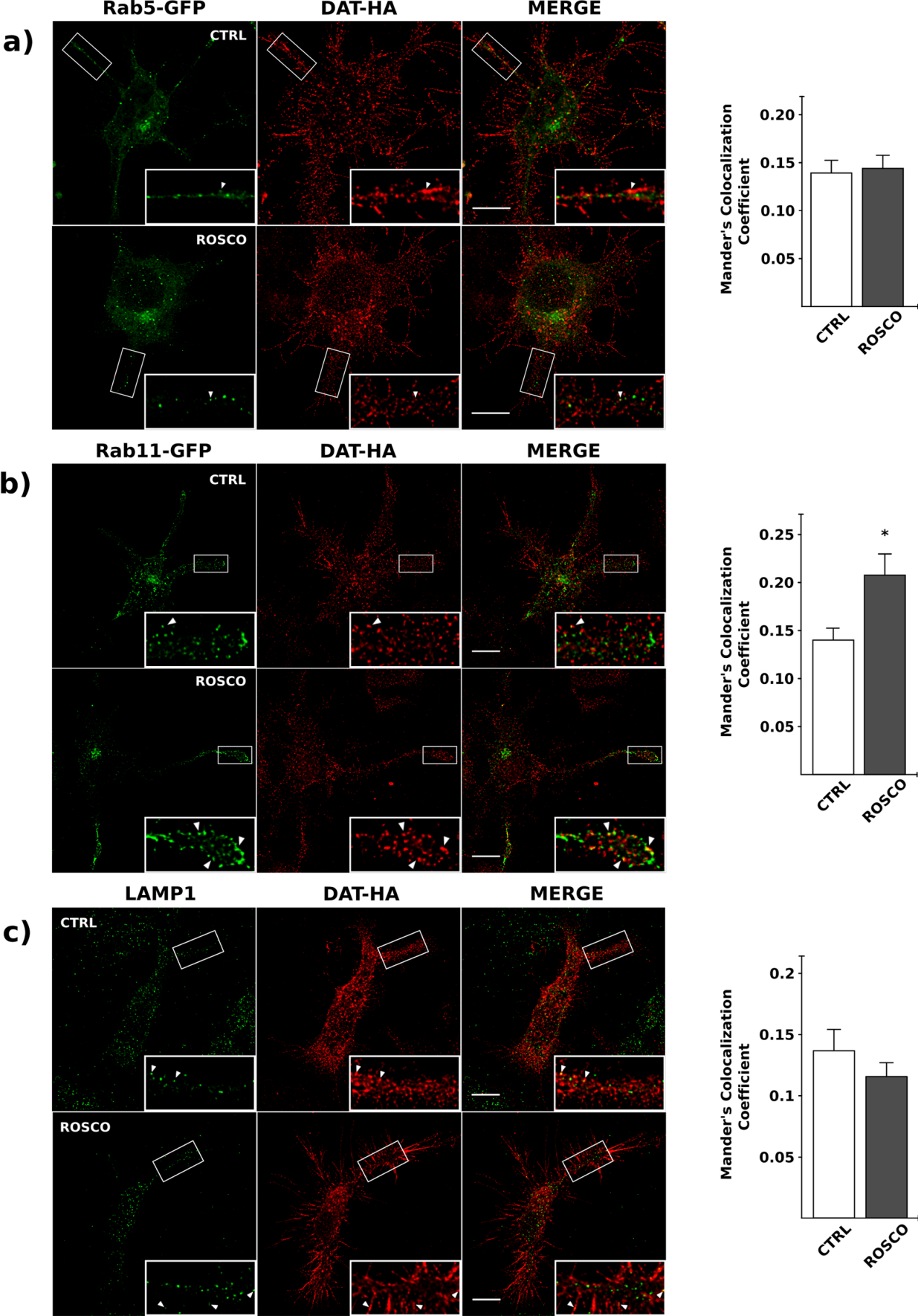
a)
Rab5-GFP
DAT-HA
MERGE
CTRL
ROSCO
Mander's Colocalization Coefficient
0.20
0.15
0.10
0.05
CTRL
ROSCO
b)
Rab11-GFP
DAT-HA
MERGE
CTRL
ROSCO
Mander's Colocalization Coefficient
0.25
0.20
0.15
0.10
0.05
*
CTRL
ROSCO
c)
LAMP1
DAT-HA
MERGE
CTRL
ROSCO
Mander's Colocalization Coefficient
0.2
0.15
0.1
0.05
CTRL
ROSCO